ChemMedChem

Chemistry Europe
European Chemical Societies Publishing

Accepted Article

Title: Facile and Improved Precursor Synthesis for the Next Generation Cardiac Positron Emission Tomography Imaging Agent [18F]Flurpiridaz

Authors: Hazem Ahmed, Ahmed Haider, Livio Gisler, Roger Schibli, Catherine Gebhard, and Simon M. Ametamey

To be cited as: *ChemMedChem* 10.1002/cmdc.202000085

Link to VoR: https://doi.org/10.1002/cmdc.202000085

WILEY-VCH

WILEY-VCH

COMMUNICATION

Facile and Improved Precursor Synthesis for the Next Generation Cardiac Positron Emission Tomography Imaging Agent [^{18}F]Flurpiridaz

Hazem Ahmed,[a] Ahmed Haider,[b, c] Livio Gisler,[a] Roger Schibli,[a] Catherine Gebhard,[b,c] and Simon M. Ametamey*[a]

[a] Dr. H. Ahmed, L. Gisler, Prof. Dr. R. Schibli, Prof. Dr. S. M. Ametamey
Institute of Pharmaceutical Sciences, Department of Chemistry and Applied Biosciences
ETH Zurich
Vladimir-Prelog-Weg 4, 8093 Zurich, Switzerland
E-mail: simon.ametamey@pharma.ethz.ch
[b] Dr. A. Haider, Prof. Dr. C. Gebhard
Department of Nuclear Medicine
University Hospital Zurich
Rämistrasse 100, 8091 Zurich, Switzerland
[c] Dr. A. Haider, Prof. Dr. C. Gebhard
Center for Molecular Cardiology
University of Zurich
Wagistrasse 12, 8952 Schlieren, Switzerland

Abstract: [^{18}F]Flurpiridaz is a recently developed positron emission tomography tracer that is currently being investigated in phase III clinical trials to measure myocardial blood flow. The relatively long physical half-life of fluorine-18 alongside the high spatial resolution and outstanding myocardium-to-background ratio fuels its potential to be the next gold standard for the early detection of coronary artery disease. Notwithstanding the expected widespread use of [^{18}F]flurpiridaz, the reported multistep synthesis of its precursor for radiofluorination involves a hazardous alkylation step using carcinogenic ethylene oxide, and a low overall chemical yield of 7%. In the current work, we improved the overall yield by more than five-fold and concurrently replaced the hazardous step. Specificity of binding of [^{18}F]flurpiridaz to mitochondrial complex 1 was demonstrated by in vitro autoradiography on mouse heart tissue sections. These results thus pave the way for assessing myocardial blood flow and coronary flow reserve in mouse models of cardiovascular disease.

Cardiovascular disease (CVD) is the leading cause of death worldwide, resulting in 17.9 million deaths amounting to 31% of all global deaths each year (World Health Organization statistics 2016). Coronary artery disease (CAD) is the build-up of plaques in the coronary heart vessels, ultimately leading to acute coronary syndromes in both women and men.[1] Resting myocardial blood flow (MBF) is the absolute amount of blood flow which the myocardium receives per minute per gram of tissue under baseline conditions. The coronary flow reserve (CFR) on the other hand is the ratio between the resting and stress MBF where this stress is typically achieved by maximal coronary vasodilation using physical or pharmacological stress agents. MBF is predominantly regulated by the microcirculation where the venules and capillary system serve as blood reservoirs holding up to 90% of the intra-myocardial blood volume.[2] CFR and MBF are affected by several factors such as age, heart rate, blood pressure, drug intake and gender.[3] Reduced CFR or MBF can be an early indicator for CAD, which can be detected by rest/stress positron emission tomography myocardial perfusion imaging (PET-MPI), non-invasively.[4] Particularly in patients with no visual sign of myocardial perfusion impairment, assessment of CFR can provide information on cardiac microvascular function.[5] PET-MPI is considered the gold standard and has inherent advantages over the more commonly used single-photon emission tomography (SPECT) MPI, such as a superior spatial and temporal resolution that allows absolute quantification of myocardial blood flow and detection of small perfusion defects. Yet its use has been limited by technical and logistical challenges.[6] Indeed, current challenges in clinical PET-MPI are nourished by the limitations of established tracers including [^{13}N]NH_3, ^{82}Rb and [^{15}O]H_2O. These PET probes suffer from exceedingly short physical half-lives ranging from 1.25 min (^{82}Rb) to 9.96 min ([^{13}N]NH_3), thus requiring either an on-site cyclotron ([^{13}N]NH_3 and [^{15}O]H_2O) or a generator (^{82}Rb). Furthermore, treadmill physical stress protocols are not practical with such short-lived radionuclides.[7] The availability of a suitable radiofluorinated PET probe will reshape the application of PET-MPI by providing an improved image quality and allowing satellite broader distribution to nuclear medicine facilities lacking an on-site cyclotron.

Mitochondria are organelles abundant in high energy-consuming organs such as the heart, rendering them an ideal target to achieve excellent signal-to-background images of the myocardium. [^{18}F]Flurpiridaz (formerly codenamed [^{18}F]BMS-747158-02), a pyridaben analogue, is a promising PET imaging radiotracer that can be used to measure absolute MBF and CFR with high accuracy.[8] Although [^{18}F]flurpiridaz binds to a specific target in the mitochondria, namely the mitochondrial complex 1 (MC-1), it can be used to quantify MBF due to the perfusion-dependent in vivo kinetics.[7, 9] Additionally the relatively long physical half-life of fluorine-18 (109.7 min) makes treadmill exercise-based imaging protocols feasible, which assesses MBF under physical stress and can therefore be used to calculate CFR.[3, 6-7] The [^{18}F]flurpiridaz myocardial uptake ratio to MBF is nearly linear (myocardial extraction fraction=94%) and correlates with different flow rates, which allows better delineation of myocardial regions with different blood flow as well as absolute quantification of MBF.[10] Compared to other PET tracers, [^{18}F]flurpiridaz has a shorter positron range resulting in the highest

image resolution, in addition to its high heart uptake to surrounding organs ratio (heart/lung 14.1 and heart/liver 8.3), thereby making it the most promising imaging tracer currently known for PET-MPI.[5b, 11] It is already showing its superiority in clinical phase III trials when compared with Tc-99m labeled SPECT MPI agents (sestamibi or tetrofosmin) and is expected to be the next benchmark for radionuclide MPI (ClinicalTrials.gov Identifier: NCT01347710).[12] To date, there is one reported synthetic route towards [^{18}F]flurpiridaz by Purohit and co-workers.[13] Despite the expected widespread use of [^{18}F]flurpiridaz, the previously reported synthesis of its tosylate precursor **13** for radiofluorination exhibits a low overall chemical yield and a hazardous alkylation step highlighted in **Scheme 1**. In the current work, we improved the overall yield by more than five-fold, while circumventing the hazardous alkylation step.

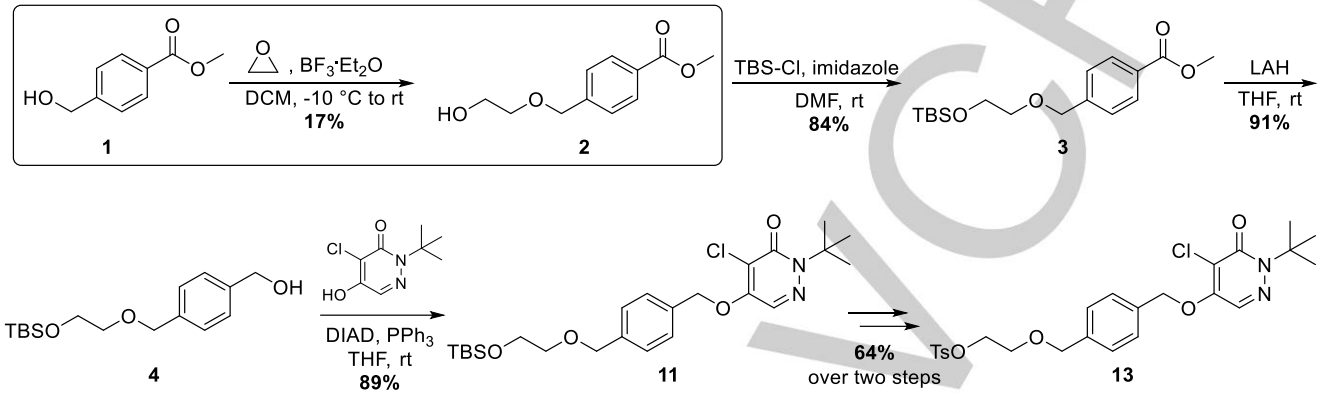

Scheme 1. Original synthesis of [^{18}F]flurpiridaz precursor.[13] The first alkylation step is the most critical and hazardous step.

Precursor **13** is not commercially available and the sole published synthetic route showed an overall yield of 7% as depicted in **Scheme 1**.[13] The synthesis of ether **2** was the biggest drawback of the entire route, owing to its poor yield of 17% and the use of ethylene oxide, a highly volatile carcinogenic toxin with reported hazardous properties in addition to difficulty in handling.[14] We envisioned retrosynthetic approaches for the synthesis of ester **3** or alcohol **4** or ether **11** as depicted in **Scheme 2.**

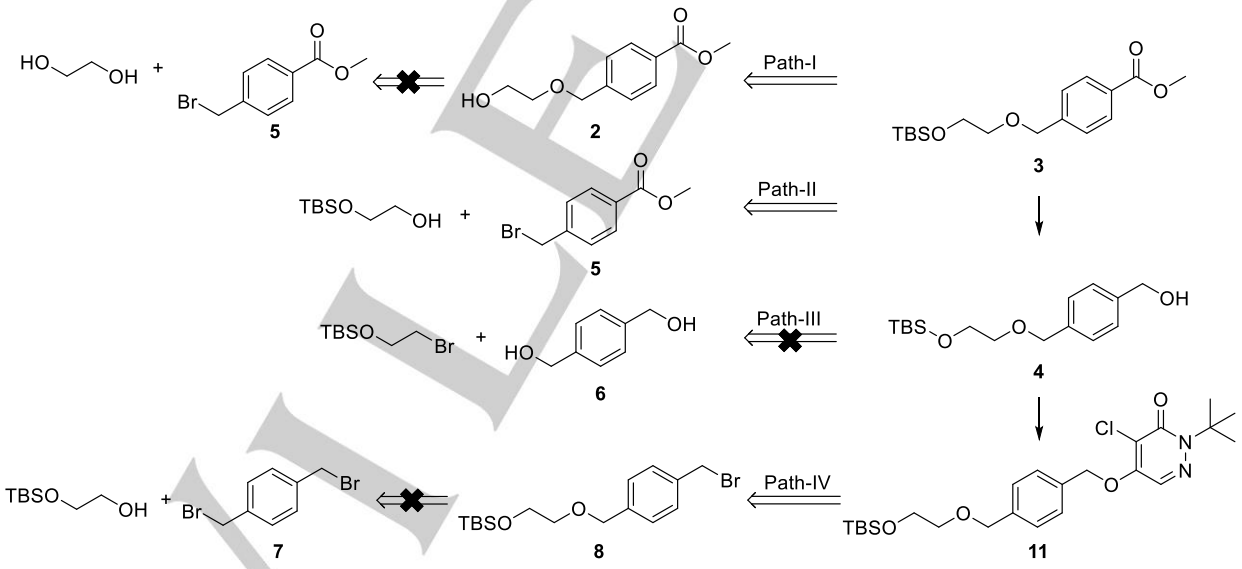

Scheme 2. Different synthetic approaches to accomplish the syntheses of ester **3** and alcohol **4**. Only path-II was feasible.

All pathways depicted were subjected to classical Williamson ether synthesis conditions using different reactant partners and sodium hydride in THF.[15] Formation of the desired product was observed only in pathway II using a mono TBS-protected ethylene glycol and benzyl bromide **5**. Additionally, we observed the formation of side-product **9** via transesterification despite varying the reaction conditions (**Scheme 3**).

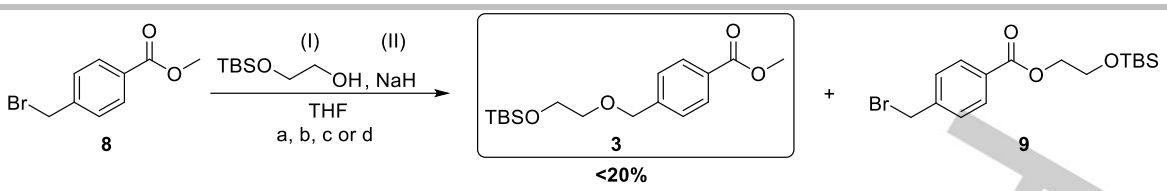

Scheme 3. Non-optimized synthetic pathway II towards intermediate **3** in <20% yields. The formation of side-product **9** was observed. Conditions: a) 6.5 equiv. (I), 0.65 equiv. (II), 1 h stirring at rt before addition of **8**, 13 h stirring at 70 °C (reflux); b) 1.1 equiv. (I), 1.1 equiv. (II), 1.5 h stirring at rt before addition of **8**, 38 h stirring at rt; c) 3.0 equiv. (I), 2.5 equiv. (II), 1 h stirring at rt before addition of **8**, 16 h stirring at 70 °C (reflux); d) 0.9 equiv. (I), 1.0 equiv. (II), 1 h stirring at rt before addition of **8**, 16 h stirring at 70 °C (reflux).

We were pleased to observe that the low <20% yields of ester **3** could be notably enhanced to 50% by the addition of a phase transfer catalyst, tetrabutylammonium iodide in DMF at 0 °C. However, the side-product **9** persisted under various reaction conditions (equivalents, temperatures and times) and this was problematic for the product separation. Therefore, we sought for an alternative solution to control the chemoselectivity of this step.

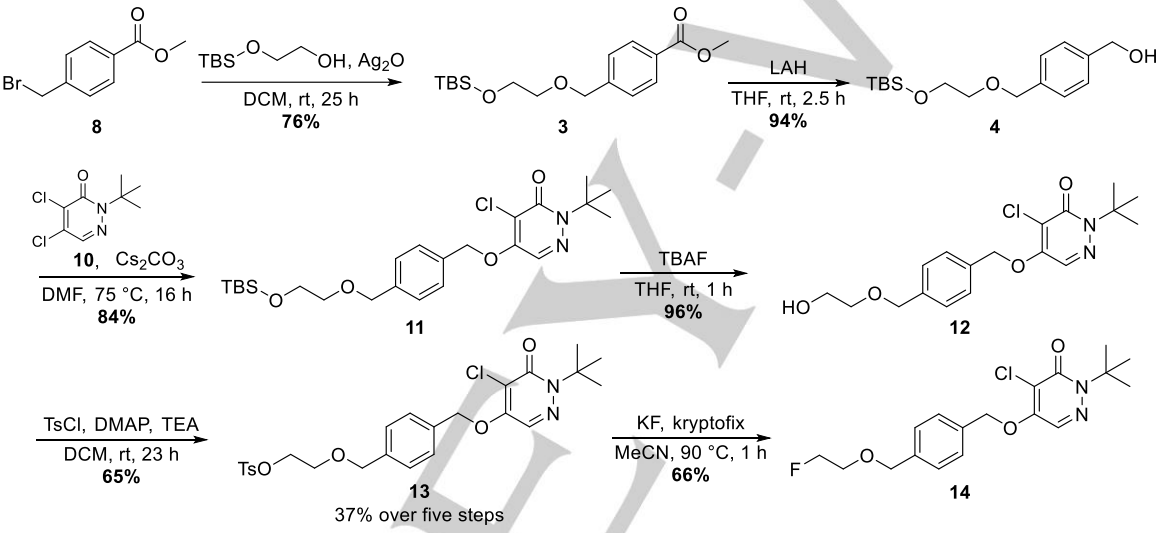

Scheme 4. Optimized synthesis route to precursor **13** and reference **14** in the current work.

The selectivity towards the bromide was greatly favoured by the use of freshly prepared silver(I) oxide, where silver coordinates with the bromide leaving group, thereby circumventing the need for a strong base or other additives. Intermediate **3** was obtained in 76% yield on a 3.5 g scale using this strategy without the formation of any detectable traces of side-product **9**. For the synthesis of intermediate **11** (**Scheme 1**), the Williamson ether synthesis conditions instead of Mitsunobu reaction were applied, given that dichloropyridazin **10** is more cost-efficient than its hydroxyl analogue. Following published procedures, the yields we obtained for compounds **12** and **13** differed from the previously reported values of 78% and 82%, respectively. We attribute this difference to the ten-fold larger amounts of reactants we used compared to Purohit et al..[13] Precursor **13** was obtained in an overall yield of 37% over five steps, which is more than five-fold higher compared to the original synthetic route of 7% yield (**Scheme 4**). In addition, this new synthetic route avoids the use of ethylene oxide, a highly volatile carcinogenic reagent with known hazardous properties. Given the expected widespread demand for [^{18}F]flurpiridaz-based PET-MPI in the near future, the availability of an appropriate and safe synthetic procedure is crucial for a wider accessibility of this exceptional probe in cardiovascular research.

Having optimized the synthetic strategy for precursor **13**, we proceeded to perform a pilot study in order to investigate the specificity of binding of [^{18}F]flurpiridaz to mitochondrial complex I in mice using mouse heart tissue sections. The radiosynthesis was carried out as previously described.[13] Autoradiograms of [^{18}F]flurpiridaz accumulation under baseline and blockade conditions are depicted in **Figure 1**.

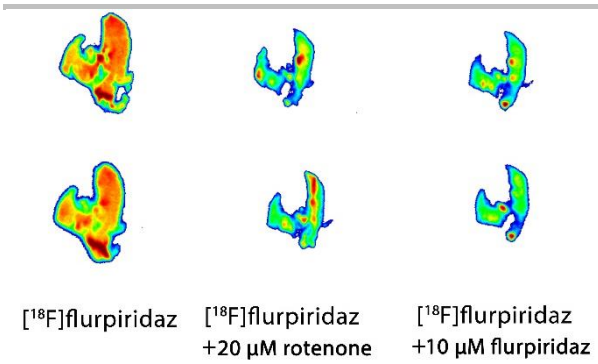

Figure 1. Representative in vitro autoradiography of mouse heart tissue sections incubated with [^{18}F]flurpiridaz under baseline and blockade conditions. Blocking was achieved with either MC-1 ligand, rotenone, or flurpiridaz.

A mean signal reduction of 68±8% (n=4) was observed following blockade with an excess of non-radioactive rotenone, a commercially available MC-1 ligand. Blockade with non-radioactive flurpiridaz resulted in comparable signal reduction (**Figure 2**), thereby confirming that [^{18}F]flurpiridaz binds specifically to MC-1 in the rodent myocardium.

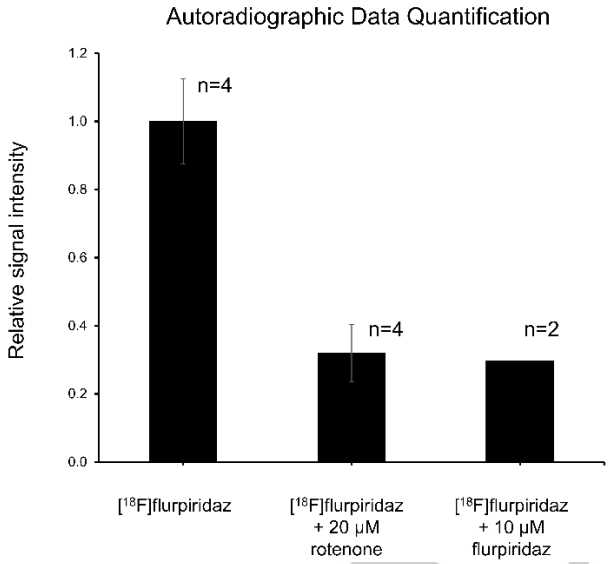

Figure 2. Quantification of specific binding of [^{18}F]flurpiridaz calculated from the in vitro autoradiographic assessment.

In summary, we have successfully synthesized precursor **13** in five steps with an overall yield of 37%, which is more than five-fold higher compared to the previously reported procedure comprising of six steps. Furthermore, the use of hazardous and toxic ethylene oxide was avoided and supplemented using readily available reagents. Our improved synthetic route is more suitable for large-scale synthesis. Using in vitro autoradiography, we also demonstrated the high specific binding of [^{18}F]flurpiridaz towards MC-1 in the mouse myocardium, thus paving the way for the assessment of MBF and CFR in various existing mouse models of cardiovascular disease.

Experimental section

Experimental procedures for the chemistry and in vitro autoradiography are presented as supplementary information.

Acknowledgments

We thank Dr. Susan Bengs for providing the rodent tissue.

Keywords: Flurpiridaz • Imaging agents • Myocardial perfusion imaging • Positron emission tomography • Synthetic methods

References

[1] a) S. K. Bhatia, in *Biomaterials for Clinical Applications*, Springer New York, New York, NY, **2010**, pp. 23-49; b) A. Haider, S. Bengs, J. Luu, E. Osto, J. M. Siller-Matula, T. Muka, C. Gebhard, *Eur. Heart J.* **2019**.

[2] A. Feher, A. J. Sinusas, *Circ Cardiovasc Imaging* **2017**, *10*, e006427.

[3] M. C. Ziadi, *Cardiovasc Diagn Ther* **2017**, *7*, 206-218.

[4] T. H. Schindler, H. R. Schelbert, A. Quercioli, V. Dilsizian, *JACC Cardiovasc. imaging* **2010**, *3*, 623-640.

[5] a) M. A. Marinescu, A. I. Loffler, M. Ouellette, L. Smith, C. M. Kramer, J. M. Bourque, *JACC Cardiovasc. imaging* **2015**, *8*, 210-220; b) B. L. Gerber, *J. Am. Coll. Cardiol.* **2012**, *60*, 1556-1557.

[6] J. Maddahi, R. R. Packard, *Semin Nucl Med* **2014**, *44*, 333-343.

[7] M. Yu, S. G. Nekolla, M. Schwaiger, S. P. Robinson, *Semin Nucl Med* **2011**, *41*, 305-313.

[8] D. S. Berman, J. Maddahi, B. K. Tamarappoo, J. Czernin, R. Taillefer, J. E. Udelson, C. M. Gibson, M. Devine, J. Lazewatsky, G. Bhat, D. Washburn, *J. Am. Coll. Cardiol.* **2013**, *61*, 469-477.

[9] P. Yalamanchili, E. Wexler, M. Hayes, M. Yu, J. Bozek, M. Kagan, H. S. Radeke, M. Azure, A. Purohit, D. S. Casebier, S. P. Robinson, *J Nucl Cardiol* **2007**, *14*, 782-788.

[10] S. G. Nekolla, S. Reder, A. Saraste, T. Higuchi, G. Dzewas, A. Preissel, M. Huisman, T. Poethko, T. Schuster, M. Yu, S. Robinson, D. Casebier, J. Henke, H. J. Wester, M. Schwaiger, *Circulation* **2009**, *119*, 2333-2342.

[11] T. Mou, X. Zhang, *Molecules* **2017**, *22*.

[12] R. Packard, J. Lazewatsky, C. Orlandi, J. Maddahi, *J. Nucl. Med.* **2017**, *58*, 369.

[13] A. Purohit, H. Radeke, M. Azure, K. Hanson, R. Benetti, F. Su, P. Yalamanchili, M. Yu, M. Hayes, M. Guaraldi, M. Kagan, S. Robinson, D. Casebier, *J. Med. Chem.* **2008**, *51*, 2954-2970.

[14] a) B. Adam, H. Bardos, R. Adany, *Mutat. Res.* **2005**, *585*, 120-126; b) C. D. Brown, B. A. Wong, T. R. Fennell, *Toxicol. Appl. Pharmacol.* **1996**, *136*, 8-19; c) J. Jinot, J. M. Fritz, S. V. Vulimiri, N. Keshava, *Toxicol. Mech. Methods* **2018**, *28*, 386-396; d) R. H. Garman, W. M. Snellings, R. R. Maronpot, *Neurotoxicology* **1985**, *6*, 117-137; e) L. Kardos, G. Szeles, G. Gombkoto, M. Szeremi, A. Tompa, R. Adany, *Environ. Mol. Mutagen.* **2003**, *42*, 59-60.

[15] R. Fenollosa, E. Garcia-Rico, S. Alvarez, R. Alvarez, X. Yu, I. Rodriguez, S. Carregal-Romero, C. Villanueva, M. Garcia-Algar, P. Rivera-Gil, A. R. de Lera, W. J. Parak, F. Meseguer, R. A. Alvarez-Puebla, *J. Nanobiotechnol.* **2014**, *12*, 35.

Table of Contents

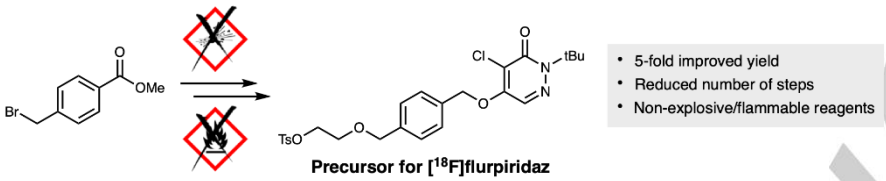

Precursor for [^{18}F]flurpiridaz

[^{18}F]Flurpiridaz is the imminent gold standard for non-invasive myocardial perfusion imaging, however, the synthetic route towards the precursor of this agent is low yielding (7%) coupled with highly hazardous and explosive chemistry, hampering access to this tracer for research and clinical applications. In the current work, we introduce a safer, less expensive and higher yielding synthetic strategy for the precursor of [^{18}F]flurpiridaz. Further, we showed 68% specific binding of [^{18}F]flurpiridaz on mice heart tissues.